Three-body resonances in pionless effective field theory

S. Dietz,[1,*] H.-W. Hammer,[1,2,†] S. König,[3,1,‡] and A. Schwenk[1,2,4,§]

[1]*Technische Universität Darmstadt, Department of Physics, 64289 Darmstadt, Germany*

[2]*ExtreMe Matter Institute EMMI and Helmholtz Forschungsakademie Hessen für FAIR (HFHF), GSI Helmholtzzentrum für Schwerionenforschung GmbH, 64291 Darmstadt, Germany*

[3]*Department of Physics, North Carolina State University, Raleigh, North Carolina 27695, USA*

[4]*Max-Planck-Institut für Kernphysik, Saupfercheckweg 1, 69117 Heidelberg, Germany*

(Received 1 October 2021; accepted 18 May 2022; published 13 June 2022)

We investigate the appearance of resonances in three-body systems using pionless effective field theory at leading order with two complementary methods. The Faddeev equation is analytically continued to the unphysical sheet adjacent to the positive real energy axis using a contour rotation. We consider both the three-boson system and the three-neutron system. For the former, we calculate the trajectory of Borromean three-body Efimov states turning into resonances as they cross the three-body threshold. For the latter, we find no sign of three-body resonances or virtual states at leading order. This result is validated by exploring the level structure of three-body states in a finite volume approach.

DOI: 10.1103/PhysRevC.105.064002

I. INTRODUCTION

The search for few-neutron resonances and bound states has a long history with ambiguous results [1,2]. In this work we focus on the topic of three-neutron resonances, motivated by a controversial discussion of this topic in the recent literature [3–10].

The first theoretical studies based on the analytical continuation of the Faddeev equation in the 1970s using a Yamaguchi-type two-neutron (nn) interaction in the ${}^1S_0$ channel found no evidence for a three-neutron resonance [11,12]. Further experiments [13–16] and theoretical investigations [17,18] did not satisfactorily resolve the situation. Theoretical studies using the complex scaling method (CSM) in the 1990s indicated a possible three-neutron resonance with an unphysically large width [19,20]. These results were supported by Ref. [21], extending Glöckle's earlier work [11] to more partial-wave channels for the nn interaction. However, subsequent theoretical investigations based on the CSM and analytical continuation in the coupling constant (ACC), again excluded a possible three-neutron resonance [22].

The interest in few-neutron resonances was revived in 2016, when experimental evidence for a four-neutron resonance was presented by Kisamori *et al.* [23]. A recent experiment even suggested that the tetraneutron could be bound [24]. A theoretical study of $3n$ and $4n$ systems suggested that these problems are connected and a three-neutron resonance might exist below a four-neutron resonance [3], which was subsequently supported by other work [7]. However, these results were criticized and led to a controversial discussion [4,6,25]. Further studies based on the Alt-Grassberger-Sandhas (AGS) equations for transition operators [5] and response functions [8] found no evidence of a three-neutron resonance. Higgins *et al.* [9,10] confirmed this further with calculations in a hyperspherical framework. They pointed out that there is significant attraction compared to free neutrons. However, because of the Pauli repulsion it does not lead to a resonance but shows up as a clear enhancement in the Wigner-Smith time delay. Other recent studies investigated the spectral properties of three-body systems near unitarity by mapping to Gaussian potentials [26], and of nuclear systems with $A = 3$–6, 16 using two- and three-body contact interactions [27]. An overview of the theoretical and experimental situation regarding few-neutron resonances was recently given in Ref. [28].

This overall situation is our motivation to investigate here the problem of three-neutron resonances using pionless effective field theory (EFT) [29–32]. Because of the relevance for Efimov states in ultracold atomic gases [33,34], we also apply our method to three-boson resonances. Pionless EFT provides a controlled, model-independent description of few-body systems with large two-body S-wave scattering length, based on an expansion in the ratio of short- and long-distance scales (see Refs. [35–38] for reviews). This description breaks down for momenta of the order of the pion mass, but is ideally suited to investigate the properties of low-energy neutron systems. It allows for a model-independent assessment of the resonance question which can be systematically improved by calculating higher orders. In the scope of pionless EFT, all higher-order corrections, including attractive P-wave channels, are perturbative. Thus we do not expect higher-order corrections to alter the low-energy resonance structure of the system. Finally,

*sebastian.dietz@physik.tu-darmstadt.de
†hans-werner.hammer@physik.tu-darmstadt.de
‡skoenig@ncsu.edu
§schwenk@physik.tu-darmstadt.de

pionless EFT describes the low-energy properties of neutron matter very well (see, e.g., Ref. [39]) and is thus ideally suited for our purpose.

In addition to an EFT framework, we need a method to investigate the resonance spectrum in this theory. The various methods for studying few-body resonances can be separated into two classes: approaches which perform calculations on the physical sheet for some form of unphysical modification of the system (altered interaction strength, adding an artificial trap), and approaches which perform calculations directly on the unphysical sheet. Both types of approaches have advantages as well as disadvantages. While the calculation on the physical sheet is simpler, the analytical continuation to the unphysical sheet can be delicate or even questionable. Direct searches of resonance poles on the unphysical sheet are much more complex, both numerically and conceptually, but generally lead to more robust results. This work uses a combination of both approaches, with a primary focus on direct calculations.

For the latter, we use the well-known Faddeev formalism [40], formulated in momentum space. Already in 1964, Lovelace proposed the method of contour rotation to analytically continue the Faddeev equation to the unphysical sheets [41]. This formalism was extended independently to general integration contours by Glöckle [11], as well as by Möller [42–46]. Furthermore, these works introduced a modified equation structure that is simpler to use. The basic idea by Lovelace of a rotated contour was extended by Pearce and Afnan and applied to several systems [47–51]. We apply this formalism in this work and note that it is conceptually equivalent to the CSM [52–56], which performs a rotation in coordinate space.[1]

We complement our direct searches for complex resonance energies by an alternative approach that falls somewhere in between the two classes of methods mentioned above. Expanding upon early work for two-body systems [59–62], Ref. [63] established that energy spectra in a periodic finite volume can be used to identify few-body resonance states as avoided crossings of energy levels as the size of the volume is varied. This method is based on the Lüscher formalism [64–66], the key insight of which is that the infinite volume S matrix governs the spectrum of a system in finite volume. An attractive feature of this method is that it does not require any contour rotation or modification of the interaction (although the finite volume bears some similarity to adding an artificial trap to confine the system). It is therefore straightforward to apply, and Ref. [63] developed an efficient discrete variable representation (DVR) to numerically calculate few-body systems in periodic boxes. A drawback of the method is that currently only resonance energies can be readily inferred from the finite-volume spectrum, while extracting information about widths requires further formal work. For our use of the method here, however, this is not a concern.

[1]An alternative formulation of resonances is given by the Berggren basis, which includes discretized resonance states explicitly in the completeness relation [57,58].

This work is structured in the following way. In Sec. II, we derive a Faddeev equation in partial-wave basis for the three-boson and three-neutron system in pionless EFT at leading order. The equation is then analytically continued to the unphysical sheet adjacent to the positive real axis in Sec. III, using a rotation of the contour of integration. Section IV applies this formalism to the three-boson and three-neutron system. For the three-boson system, we calculate the resonance energy and width for a broad range of negative scattering length and compare to results in the literature. We show that no three-neutron bound state is possible and calculate the pole trajectory on the unphysical sheet for a bound two-neutron subsystem. Searching for resonance poles and virtual states for an unbound subsystem up to the physical nn scattering length, no indications for resonances or virtual states in the $J^\pi = \frac{1}{2}^-$, $\frac{3}{2}^-$, and $\frac{1}{2}^+$ channels are found. In Sec. V, we discuss the complementary finite-volume formalism to extract resonance properties from avoided level crossings in finite volume energy spectra. No evidence of avoided level crossings for the negative parity states is found, confirming the Faddeev results for the $J^\pi = \frac{1}{2}^-$ and $\frac{3}{2}^-$ channels. Finally, a summary and outlook are given in Sec. VI.

We emphasize that the novel aspect of our work lies in the use of a model-independent pionless EFT approach, which is systematic and transparent. Moreover, our study is carried out using two complementary methods with different systematics: resonance trajectories in the complex plane and finite-volume calculations.

II. FADDEEV FORMALISM

Since we work in the Faddeev formalism, we follow Refs. [67,68] and use pionless EFT [29–32] to construct an effective interaction potential,

$$V_{\text{eff}} = \sum_{n=2}^{\infty} V_n, \tag{1}$$

where the index n specifies an n-body potential. In general, interaction terms up to $n = N$ contribute in a N-body problem, but at low energies higher-body terms are typically suppressed. The potentials V_n are constrained by Galilean invariance and thus depend only on the relative momenta. They can be expressed in a momentum expansion, e.g.,

$$\langle \mathbf{k}'|V_2|\mathbf{k}\rangle = C_0 + C_2(\mathbf{k}'^2 + \mathbf{k}^2)/2 + \cdots \tag{2}$$

for S-wave two-body interactions, where $\mathbf{k}$ and $\mathbf{k}'$ are the relative momenta in the initial and final states and regulator functions have been suppressed. Similar expressions can be derived for three- and higher-body interactions. At leading order in pionless EFT, only a momentum-independent two-body contact interaction in the ${}^1S_0$ channel contributes for the three-neutron system [69,70]. In the three-boson system, in contrast, an additional momentum-independent three-body contact interaction has to be included to properly renormalize the system [71,72]. Assuming typical momenta of order $1/a$, the uncertainty of a leading-order pionless EFT calculation can be estimated as $|r/a|$, where r is the effective range and a the scattering length. For the

three-neutron system, we have $a \approx -18.9$ fm and $r \approx 2.7$ fm [73], such that a leading-order calculation has an uncertainty of about 15%. Thus the higher-order corrections are not expected to change the resonance structure of the system. The exact form of the effective potential depends on the specific regularization scheme used. The low-energy observables, however, are independent of the regularization scheme (up to higher-order corrections) and one can choose a convenient scheme for practical calculations. Explicit forms for the effective potentials will be given below. (For a more detailed discussion of pionless EFT including a more formal discussion of the power counting, we refer to the reviews [35–38].)

Our starting point for deriving the Faddeev equations is the full relative three-body wave function $|\Psi\rangle$, defined as a solution of the stationary Schrödinger equation. This wave function is decomposed into the three so-called Faddeev components $|\psi_i\rangle$ according to

$$|\Psi\rangle = \sum_{i=1}^{3} |\psi_i\rangle \equiv G_0 \left(\sum_{i=1}^{3} V_2^{(i)} + V_3 \right) |\Psi\rangle, \tag{3}$$

where $i = 1, 2, 3$ labels the three different pairs in the three-body system. The above definition includes the free Green's function

$$G_0(z) = \frac{1}{z - H_0}, \tag{4}$$

where z is an arbitrary (in principle complex) energy. H_0 represents the relative kinetic part of the Hamiltonian and the two-body pair interactions are given by $V_2^{(i)}$. Moreover, a three-body force V_3 is included here as well to keep the equation sufficiently general for the three-boson and three-neutron systems.

Introducing the permutation operator

$$P = P_{12}P_{23} + P_{13}P_{23}, \tag{5}$$

we are able to express the full state by only one component,

$$|\Psi\rangle = (1 + P)|\psi_1\rangle. \tag{6}$$

The index 1 is dropped in the following.

Altogether, the leading-order representation of the Faddeev equation is given by [74]

$$|\psi\rangle = G_0 t P |\psi\rangle + \tfrac{1}{3}(G_0 + G_0 t G_0) V_3 (1 + P)|\psi\rangle. \tag{7}$$

The S-wave two-body interaction V_2 is chosen as

$$\langle k'|V_2|k\rangle = C_0 \langle k'|g\rangle\langle g|k\rangle, \tag{8}$$

with strength C_0, $k = |\mathbf{k}|$, and $k' = |\mathbf{k}'|$. It is included via the two-body T matrix t which satisfies the Lippmann-Schwinger equation. We use a Gaussian type regulator function

$$\langle p|g\rangle = g(p) = \exp(-p^2/\Lambda^2), \tag{9}$$

where Λ is the cutoff scale. This form is particularly convenient for the analytic continuation of the formalism into the complex plane. For the finite-volume calculations discussed in Sec. V, we will also consider super-Gaussian regulators, which fall off faster at large momenta, to improve the convergence.

The three-body potential is parametrized as

$$V_3 = D_0 |\xi\rangle\langle\xi|, \tag{10}$$

with the interaction strength D_0 and the three-body regulator $|\xi\rangle$. We again choose a (separable) Gaussian regulator function, connected to the two-body regulator by

$$\langle u_1 u_2|\xi\rangle = \xi(u_1, u_2) = g(u_1) g\left(\frac{\sqrt{3}}{2} u_2\right), \tag{11}$$

where

$$\begin{aligned} \mathbf{u}_1 &= \tfrac{1}{2}(\mathbf{k}_1 - \mathbf{k}_2), \\ \mathbf{u}_2 &= \tfrac{2}{3}\left[\mathbf{k}_3 - \tfrac{1}{2}(\mathbf{k}_1 + \mathbf{k}_2)\right] \end{aligned} \tag{12}$$

are three-body Jacobi momenta. Here, $\mathbf{u}_1$ represents the relative momentum between the first two particles, while the relative momentum between the third particle and the center of mass of the first two particles is given by $\mathbf{u}_2$. The relative kinetic energy of the three-body system is given by

$$H_0|\mathbf{u}_1\mathbf{u}_2\rangle = \left(u_1^2 + \tfrac{3}{4}u_2^2\right)|\mathbf{u}_1\mathbf{u}_2\rangle. \tag{13}$$

Here and in the following, we set $m = 1$ such that energy and momentum squared have the same units. Together with the appropriate angular momentum, spin, and isospin quantum numbers, which are summarized in the multi-index $|i\rangle$, we define our basis as $|u_1 u_2 i\rangle$.

This work uses a jj coupling scheme, for which the set of quantum numbers is given by

$$|i\rangle = |(ls)j(\lambda s_3)IJ\rangle, \tag{14}$$

with the relative orbital angular momentum l between the first two particles and the orbital angular momentum λ relative to the third particle. s is the coupled spin of the first two particles, which couples with l to j. Similarly, the spin of the third particle s_3 couples with λ to I, which itself is coupled with j to the total angular momentum J.

We now derive the equations for both the three-neutron and three-boson systems in parallel. For definiteness, we consider a system of three spinless bosons, where

$$|i\rangle = |(00)0(00)00\rangle. \tag{15}$$

In the case of the three-neutron system, we suppress the isospin quantum number 3/2, while the three-body force is absent because the Pauli principle precludes a momentum-independent contact three-neutron force.[2] To leading order in pionless EFT, only S-wave two-body interactions contribute. We consider the basis states

$$|i\rangle = \left|(00)0\left(1\tfrac{1}{2}\right)\tfrac{3}{2}\tfrac{3}{2}\right\rangle, \tag{16}$$

which correspond to $J^\pi = \frac{3}{2}^-$, and

$$|i\rangle = \left|(00)0\left(\lambda\tfrac{1}{2}\right)\tfrac{1}{2}\tfrac{1}{2}\right\rangle, \tag{17}$$

[2]Three-neutron forces including derivatives would be permitted, but they only enter at higher orders in the EFT power counting.

for the cases $\lambda = 0, 1$, which correspond to $J^\pi = \frac{1}{2}^+, \frac{1}{2}^-$. As will be shown below, the Faddeev equations for $\lambda = 1$ are the same and will be investigated simultaneously. In all cases, the Faddeev equations reduce to a single channel, and consequently the index i will be dropped in the following.

Now we are able to derive the three-body partial-wave projected Faddeev equation by projecting (7) onto the single-channel basis. We exploit the fact that the free Green's function G_0 is diagonal in all variables,

$$\langle u_1' u_2' | G_0(E) | u_1 u_2 \rangle = G_0(E; u_1, u_2) \frac{\delta(u_1' - u_1)}{u_1' u_1} \frac{\delta(u_2' - u_2)}{u_2' u_2}, \tag{18}$$

with

$$G_0(E; u_1, u_2) = \left(E - u_1^2 - \tfrac{3}{4} u_2^2\right)^{-1}. \tag{19}$$

The two-body t-matrix can be written as

$$\langle u_1' u_2' | t(E) | u_1 u_2 \rangle = g(u_1') \tau(z) g(u_1) \frac{\delta(u_2' - u_2)}{u_2' u_2}, \tag{20}$$

with the energy of the first pair of particles $z = E - \frac{3}{4} u_2'^2$. Within the EFT formalism τ describes the propagation of an interacting two-particle state, commonly called a "dimer." Following this convention, we refer to τ as the dimer propagator. Together with the explicit representation of the three-body interaction (10), the Faddeev equation can be written as

$$\begin{aligned} \psi(u_1 u_2) = G_0(E; u_1, u_2) \Bigg[& \int_{-1}^{+1} dx \int du_2' u_2'^2 \, g(u_1) \tau\left(E - \frac{3}{4} u_2^2\right) g(\pi_1) G(u_2 u_2' x) \langle \pi_2 u_2' | \psi \rangle \\ & + D_0 \int du_1' u_1'^2 \int du_2' u_2'^2 \, \xi(u_1', u_2') \langle u_1' u_2' | \psi \rangle \Bigg\{ \xi(u_1, u_2) + g(u_1) \tau\left(E - \frac{3}{4} u_2^2\right) \\ & \times \int du_1'' u_1''^2 \, \xi(u_1'', u_2) G_0(E; u_1'', u_2) g(u_1'') \Bigg\} \Bigg]. \end{aligned} \tag{21}$$

Note that the factor $1 + P$ within Eq. (7) cancels against the factor $1/3$. Here we have used the matrix element of the permutation operator

$$\langle u_1' u_2 | P | u_1'' u_2'' \rangle = \int_{-1}^{+1} dx \frac{\delta(u_1' - \pi_1)}{u_1'^2} \frac{\delta(u_1'' - \pi_2)}{u_1''^2} G(u_2 u_2'' x), \tag{22}$$

with

$$\pi_1 = \sqrt{u_2''^2 + \frac{1}{4} u_2^2 + u_2 u_2'' x}, \tag{23}$$

$$\pi_2 = \sqrt{\frac{1}{4} u_2''^2 + u_2^2 + u_2 u_2'' x}. \tag{24}$$

In general, the recoupling function $G(u_2 u_2'' x)$ depends on both momenta and angular quantum numbers. Besides the two-body t-matrix, it is this term that mainly incorporates the information about the quantum numbers of the system. It reduces to the Legendre polynomial P_0 for the three-boson system,

$$G_{3\mathrm{b}}(u_2 u_2'' x) = P_0(x) = 1, \tag{25}$$

and to a constant times a Legendre polynomial for the three-neutron system,

$$G_{3\mathrm{n}}^{\lambda}(u_2 u_2'' x) = -\tfrac{1}{2} P_\lambda(x), \tag{26}$$

for $\lambda = 0, 1$. Finally, the dimer propagator τ can be written as

$$\tau(z) = \left[\frac{1}{C_0} - I(z)\right]^{-1}, \quad \text{with}$$

$$I(z) = \langle g | G_0(z) | g \rangle = \int_0^\infty dq \, q^2 \frac{g(q) g(q)}{z + i\varepsilon - q^2}. \tag{27}$$

Solving the integral $I(z)$ analytically results in

$$\begin{aligned} \tau(z) &= \frac{2}{\pi} \left[\gamma \exp\left(2 \frac{\gamma^2}{\Lambda^2}\right) \mathrm{erfc}\left(\frac{\sqrt{2}|\gamma|}{\Lambda}\right) \right. \\ &\quad \left. + i\sqrt{z} \exp\left(-2 \frac{z^2}{\Lambda^2}\right) \mathrm{erfc}\left(\mp i \frac{\sqrt{2z}}{\Lambda}\right) \right]^{-1} \\ &= \frac{2}{\pi} [\gamma + i\sqrt{z} + \mathcal{O}(\Lambda^{-1})]^{-1}. \end{aligned} \tag{28}$$

The upper (lower) sign corresponds to the case $\mathrm{Im}\, z > 0$ ($\mathrm{Im}\, z < 0$), while $\mathrm{erfc}(z)$ represents the complementary error function,

$$\mathrm{erfc}(z) = 1 - \mathrm{erf}(z) = \frac{2}{\sqrt{\pi}} \int_z^\infty dt \, e^{-t^2}. \tag{29}$$

The representation in the first line of Eq. (28) includes finite-range contributions induced by the finite cutoff Λ. The expressions in the first and second line are equivalent in the limit $\Lambda \longrightarrow \infty$. Within this work we use the representation in the second line because it provides a simpler analytic continuation to complex resonance energies. We renormalize the dimer propagator by choosing C_0 to reproduce a pole in the two-body subsystem at $\sqrt{z} = i\gamma$. For positive γ, we reproduce a two-body bound state at $E_2 = -\gamma^2 = -1/a^2$, with the two-body binding momentum γ and the scattering length a. For negative γ, we reproduce the corresponding virtual state.

Finally, since we are working with separable interactions, it is convenient to transform the Faddeev equations by defining

$$\psi(u_1, u_2) = G_0(E; u_1, u_2) g(u_1) \tau\left(E - \tfrac{3}{4} u_2^2\right) F(u_2), \tag{30}$$

where $F(u_2)$ is the so-called reduced Faddeev component. Instead of the full Faddeev component the reduced

component only depends on one momentum variable, reducing the numerical effort to solve the problem.

A. Three-boson equation

Combining all contributions presented above, the Faddeev equation representing the three-boson system is given by

$$F(u_2) = \int du_2' \, u_2'^2 \, \tau(z)(Z_2 + Z_3)F(u_2'). \tag{31}$$

In analogy to the Lippmann-Schwinger equation, we define a two-body interaction kernel

$$Z_2 = \int_{-1}^{+1} dx \, g(\pi_1) G_0(E; \pi_2, u_2') g(\pi_2) \tag{32}$$

with $z = E - \frac{3}{4}u_2'^2$ and three-body interaction kernel

$$Z_3 = \frac{D_0}{C_0} g\left(\frac{\sqrt{3}}{2}u_2\right) g\left(\frac{\sqrt{3}}{2}u_2'\right) I\left(E - \frac{3}{4}u_2'^2\right). \tag{33}$$

While Z_3 arises from the three-body force, Z_2 is the contribution from the one-particle exchange.

B. Three-neutron equation

Finally, we adapt the equation to the three-neutron system. Due to the Pauli principle only an S-wave nn interaction in the ${}^1S_0$ channel is possible. The exact value of the nn scattering length is still debated, but the currently accepted value is (-18.9 ± 0.4) fm [73]. The third neutron is to be assumed in a relative P wave ($\lambda = 1$) in accordance with previous studies. This results in the possible states $J^\pi = \frac{1}{2}^-$ and $\frac{3}{2}^-$, which are degenerate in leading-order pionless EFT. These are the most likely channels for three-neutron resonances to occur [28]. The corresponding Faddeev equation reads

$$F(u_2) = -\frac{1}{2} \int du_2' u_2'^2 \int_{-1}^{+1} dx \, g(\pi_1) G_0(E; \pi_2, u_2') \times g(\pi_2) P_1(x) \tau\left(E - \frac{3}{4}u_2'^2\right) F(u_2'). \tag{34}$$

Moreover, we consider the case of the third neutron in a relative S wave ($\lambda = 0$), corresponding to $J^\pi = \frac{1}{2}^+$. The resulting Faddeev equation is derived from Eq. (34) by replacing $P_1(x)$ by $P_0(x) = 1$. In contrast to the three-boson system, the three-neutron equations feature no three-body forces since such terms are highly suppressed for identical fermions. This is taken into account by setting D_0 to zero.

III. ANALYTICAL CONTINUATION: METHOD

Due to the square root connection between the energy and the momentum variables, two points in the complex momentum plane are mapped onto a single point in the complex energy plane. This mapping is made unique by introducing a two-sheet structure for the energy variable. Solving the Faddeev equations for the three-body system, it is straightforward to search for bound states located on the first (or "physical") sheet of the complex energy plane. In this work, however, we are interested in resonances and virtual states, which live on the second ("unphysical") sheet.

The procedure described in the following assumes a three-body system of identical particles, for which the two-body subsystems are not bound. It can easily be extended to bound subsystems by considering the complex energy and momentum planes relative to the two-body threshold. We note that the formalism can also be applied to systems of nonidentical particles. This leads to a more complicated sheet structure due to further thresholds. In this work, however, we need not deal with this complication.

We start at a three-body bound state $E^{(0)}$ for an (unphysical) scattering length $a^{(0)} > 0$ and investigate the pole trajectory in the complex momentum plane as a function of the scattering length. In systems of ultracold atoms, these trajectories can be followed experimentally using Feshbach resonances [75]. Figure 1 shows a sketch of such a trajectory in the relevant region of the complex momentum plane.

A characteristic point of this trajectory is the origin, which corresponds to a so-called branch point. Two sheets are connected by a branch cut, which is spanned between two branch points. The first method used in this paper to search for resonances is to analytically continue the Faddeev equations derived in the previous chapter through this cut onto the adjacent unphysical sheet.

In the Faddeev equations a cut can originate from either of two characteristic structures in the kernel: On the one hand, there is the dimer propagator, Eq. (28). This square-root branch cut is not relevant for this work as it is only present for bound two-body subsystems. On the other hand, the kernel includes the one-particle exchange contribution given in Eq. (32). The relevant structure is the free Green's function

$$G_0(E; \pi_2, u_2') = \left[E - u_2^2 - u_2'^2 - u_2 u_2' x\right]^{-1}. \tag{35}$$

It generates a branch cut, the so-called three-body cut, between the branch point at the origin ($u_2 = u_2' = 0$) and the second branch point at infinity in the limit $u_2, u_2' \longrightarrow \infty$. Applying the partial-wave projection by integrating over x results in a logarithmic structure. Similarly to the square root, the complex logarithm is a multivalued function: it does not change if an integer multiple of $2\pi i$ is added to its argument. Therefore, this branch cut leads to an infinite number of unphysical sheets. Physically, only the one adjacent to the lower rim of the physical sheet is relevant as it affects measurable quantities such as the cross section.[3]

Assuming the pole moves through the cut onto the physically relevant unphysical sheet, we have to analytically continue the Faddeev equations to momenta with a negative imaginary part and a positive real part, i.e., to complex momenta in the lower right quadrant of the complex plane. The analytical continuation is based on the general idea of writing down a Faddeev-like equation with a contour of integration on the unphysical sheet. This procedure moves the location of the cut and thereby makes part of the second sheet accessible via the standard Faddeev equation, i.e., an equation that is

[3]Note that the regulator can generate also an artificial cut. However, the contact interaction with separable Gaussian regulator used here does not generate any singularities.

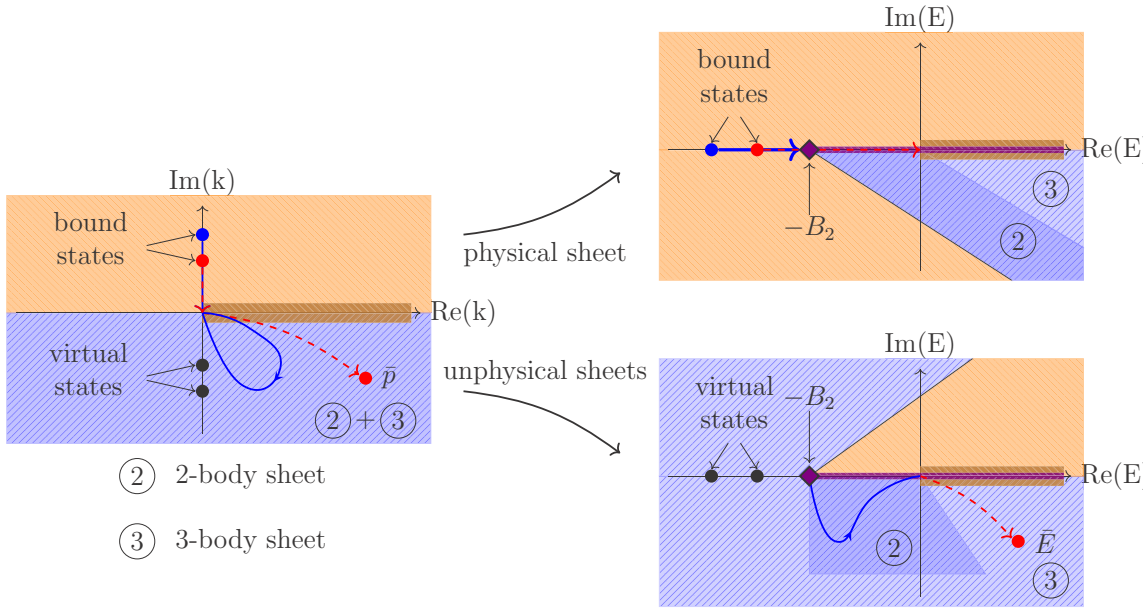

FIG. 1. The structure of the complex momentum and energy plane for three particles defined by the energy-momentum relation $E = \frac{3}{4}k^2 - B_2$, where B_2 is the two-body binding energy. Energies on the physical sheet (upper right plot) translate to momenta on the physical part of the momentum plane with $\mathrm{Im}(k) > 0$ (shading ▨). Energies on the unphysical sheets (lower right plot) are mapped to the region of the complex momentum plane with $\mathrm{Im}(k) < 0$ (shading ▨). The physical and unphysical sheets are connected by two branch cuts; the three-body cut starting at the origin and following the positive real axis and the two-body cut starting at the two-body binding energy B_2 (◆) and following the real axis, too. The complex energy plane shows two unphysical sheets: the one accessible through the cut starting at the two-body threshold (2-body sheet, darker shaded) and the one accessible through the three-body threshold (3-body sheet, lighter shaded). Both unphysical sheets extend further than sketched here. While bound states are located on the physical sheet, virtual states and resonances $\bar{p}/\bar{E}$ live on the unphysical sheets. This is also true for the corresponding areas on the complex momentum plane. The pole trajectories as a function of the two-body interaction strength of the three-boson system ($a < 0$, dashed lines) and three-neutron system using the Yamaguchi model (solid lines) are sketched. Starting at a given bound state and decreasing the two-body interaction strength the three-boson system moves through the three-body branch point, as the two-boson system is unbound, and evolves into a resonance. The Yamaguchi model allows to create a bound two-neutron subsystem, of which the binding energy decreases slower than the three-neutron binding energy. At some point both values are equivalent and the pole trajectory moves through the two-body cut onto the unphysical sheet. Finally, the two as well as the three-neutron pole trajectory meet again at the origin. Note that the position of the two-body branch point depends on the two-body interaction strength. So its position is different for every point along the pole trajectory.

formally the same as before except that the integral runs along the contour in the complex plane. Using this equation, all poles, which are located between the rotated contour (which coincides with the rotated branch cut) and the positive real axis can be identified. Generally, there are an infinite number of possible contours. However, it is sufficient in practice (and convenient) to use just one particular type of contour, which was first applied to this problem by Pearce and Afnan [47]. The contour is constructed by rotating the integral from the positive real axis, $[0, \infty)$, into the lower right quadrant,

$$u_2' \longrightarrow u_2' \, e^{-i\varphi}, \quad \varphi > 0. \tag{36}$$

The benefit of this contour is that it is rather simple and characterized by only one parameter, the rotation angle φ.[4] This angle has to be chosen such that the cut is rotated beyond the position of the state of interest (cf. Fig. 2). This statement is equivalent to the condition

$$\varphi > \Phi = \arctan \left| \frac{\mathrm{Im}\, \bar{p}}{\mathrm{Re}\, \bar{p}} \right|. \tag{37}$$

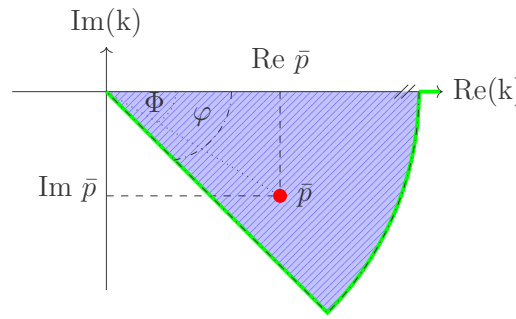

FIG. 2. The part of the unphysical region adjacent to the three-body cut, which is available if the angle of rotation is chosen to be φ. The angle has to be larger than the angle Φ of a possible state $\bar{p}$ on that sheet.

[4]In principle this contour should be constructed by rotating a finite interval (say, $[0, \Lambda]$) and then closing it towards the real axis at the end point. However, we assume here that the contribution from the arc becomes irrelevant in the limit $\Lambda \to \infty$.

The key requirement of this formalism is that the kernel of the Faddeev equation is analytic within the momentum region covered by the contour rotation. First, we have to show that these type of contours can be used without encountering a singularity. As explained before, we here need only take into account poles of the one-particle exchange contribution. Considering the momentum plane of the integration variable u_2', we choose momenta u_2 along the contour of integration for a fixed energy E. This results in two areas in which the kernel is not analytic in [11]. The general procedure is to start with an energy on the physical sheet and show that the contour of integration can be deformed in such a way that eventually the interesting part of the unphysical sheet becomes accessible without hitting any one of the singular areas. This process takes place in repeated steps. First, the contour is rotated as far as possible. Then, the energy is moved as far as possible, too. These steps are repeated as often as necessary.

Further, we have to require that the momentum of the first pair of particles k is continuous within the momentum plane. Again, we start at a bound state $E^{(0)} < 0$ on the physical sheet. So, we apply the three-boson or three-neutron Faddeev equation with the integration contour along the positive real axis ($u_2'^2 \in \mathbb{R}^+$). Here, k is defined by

$$\begin{aligned} k = \sqrt{z} &= \sqrt{E - \frac{3}{4}u_2'^2 + i\varepsilon} \\ &= i\sqrt{-E + \frac{3}{4}u_2'^2 - i\varepsilon}. \end{aligned} \tag{38}$$

Both representations of the square root are equivalent and the $i\varepsilon$ term is explicitly needed to determine the correct branch.

Now, we move to the unphysical sheet of interest with $E, u_2'^2 \in \mathbb{C}$ and $\mathrm{Im}\, E, \mathrm{Im}\, u_2' < 0$. Here, the $i\varepsilon$ is not necessary anymore and we drop it. So, also the two representations are no longer equivalent. Choosing u_2' along the contour of integration and E within the fourth quadrant of the complex energy plane where the resonances live, we have to check that k does not cross any cut. This is only the case for one of the two representations. Choosing $\varphi = \Phi$ the argument of both representations crosses the real axis at the origin. As mentioned above, we choose $\varphi > \Phi$. So, the argument of the first representation crosses the real axis at positive real parts, while the second representation crosses the axis at negative imaginary parts. The complex square root is a two-branched function. Both branches are connect at the negative real axis. The second representation would cross the square-root branch cut, while the first does not. So, for energies in the fourth quadrant we have to use the first representation. A similar investigation shows that also for energies in the third quadrant the first representation is the one to use. Note that these statements are only correct for an unbound two-body subsystem. If the subsystem is bound we have to consider the energy plane which is shifted by the two-body binding energy. This results in a dependence of the rotation angle on the two-body binding energy.

Altogether, the analytically continued Faddeev equation for the three-boson system is given by Eq. (31) with τ given by Eq. (28) and the contour rotation Eq. (36),

$$\begin{aligned} F(u_2 e^{-i\varphi}) = \int du_2'\, u_2'^2 e^{-3i\varphi}\, \tau(z) \\ \times\ (Z_2 + Z_3) F(u_2' e^{-i\varphi}). \end{aligned} \tag{39}$$

Applying the same modifications to Eq. (34), the analytically continued three-neutron equation for $\lambda = 1$ is given by

$$\begin{aligned} F(u_2 e^{-i\varphi}) = -\frac{1}{2} \int du_2'\, u_2'^2 e^{-3i\varphi} F(u_2' e^{-i\varphi}) \\ \times \int_{-1}^{+1} dx\, g(\pi_1 e^{-i\varphi}) g(\pi_2 e^{-i\varphi}) P_1(x) \\ \times\ G_0(E; \pi_2 e^{-i\varphi}, u_2' e^{-i\varphi}) \tau(z). \end{aligned} \tag{40}$$

The corresponding equation for $\lambda = 0$ is obtained by substituting $P_1(x) \to 1$ in Eq. (40).

Finally, let us add a remark on the solution of the Faddeev equations. The mathematical structure of the inhomogeneous Faddeev equation for the T matrix is given by a so-called Fredholm equation of the second kind. On the physical sheet the kernel is Hermitian and it can be shown that the T matrix can be expanded in a basis given by the reduced Faddeev components. The coefficients of the expansion are proportional to 1 over $1 - \lambda_n$, with the eigenvalues of the homogeneous Faddeev equation λ_n. This expansion was extended to non-Hermitian kernels by Afnan [48]. So, to find poles on the unphysical sheet we have to search for eigenvalues equal to one of the Faddeev equations for the reduced Faddeev components along the rotated contour. The first step of the procedure is now similar to the search for a bound state on the physical sheet. We expand the kernel in a momentum space basis derived by a Gauss-Legendre mesh. Now, these momenta are substituted by the rotated momenta. Here, also the weight in the integral has to be transformed correctly. Following the expansion, the next step would be to search for eigenvalues equal to one as a function of the complex energy. However, mathematically equivalent but numerically easier and faster is the search for zeros of the characteristic polynomial for eigenvalues equal to 1. In comparison to the search for a bound-state pole this corresponds to two-dimensional root finding. Mathematically, this is much more advanced and it cannot be guaranteed that the corresponding numerical routines will find all poles. So, before applying the root-finding routines it is recommended to plot the absolute value of the characteristic polynomial as a function of the complex energy. This plot largely depends on the numerical parameters used within the derivation of the kernel matrix. The only physically relevant part are the zeros, which are used as starting values for the root-finding routines.

IV. ANALYTICAL CONTINUATION: RESULTS

We now discuss our results from the analytical continuation, first for the three-boson case, where we can compare to previous studies of resonances to benchmark our method, and then for the three-neutron case.

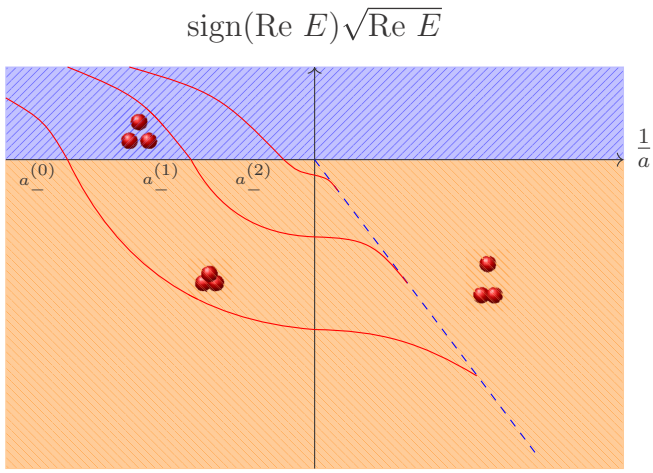

FIG. 3. The so-called Efimov plot presenting the Efimov effect. The x axis presents the inverse scattering length, while the y axis shows the square root of the real part of the energy multiplied by its sign. The dashed-blue line indicates the binding energy of the dimer $B_2 = 1/a^2$. In the area right to the dashed blue line the three-body system is unbound, while the dimer is bound. Crossing the line, the three-body system becomes bound too until a negative scattering length $a_-^{(n)}$ is reached. Here, the pole moves from the physical sheet (light shaded) to the unphysical sheet adjacent the positive real axis (dark shaded) becoming a resonance.

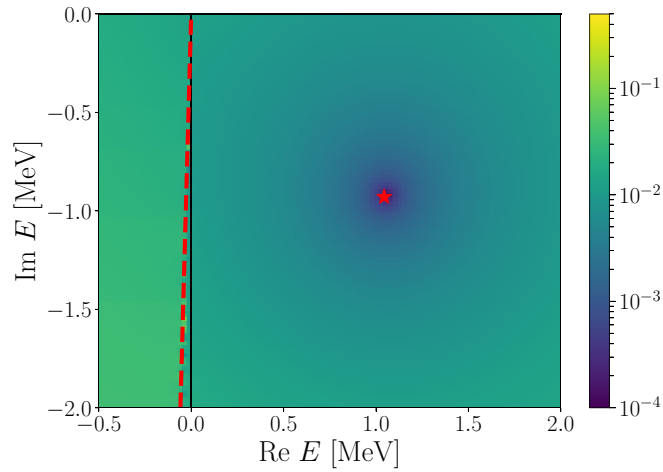

FIG. 4. The absolute value of the characteristic polynomial for a scattering length $a = -2.47$ fm (chosen arbitrarily) on the unphysical sheet adjacent to the three-body cut. The calculation is performed using a rotation angle $\varphi = 0.8$ rad (45.84°). As a consequence the three-body cut (dashed line) appears at an angle $2\varphi = 1.6$ rad (91.67°), close to the negative imaginary axis. The value where the characteristic polynomial becomes zero is indicated by a star, which corresponds to a three-boson resonance. Similar plots can be created for the other scattering length values along the pole trajectory.

A. Three-boson system

The three-boson system for large scattering length exhibits the so-called Efimov effect [33,76]. It leads to a universal spectrum of three-body bound states which is illustrated in Fig. 3. There is a more general discrete scaling symmetry which relates the trajectory of any three-body bound state to all other states via the transformation

$$\begin{aligned} a &\longrightarrow \nu^n a, \\ E &\longrightarrow \nu^{-2n} E, \end{aligned} \tag{41}$$

where n is an integer and $\nu \approx 22.7$ is the discrete scaling factor. In the unitary limit ($a \longrightarrow \pm\infty$) the binding energies of two consecutive states are connected by

$$E_{n+1} = \nu^2 E_n. \tag{42}$$

Here, the counting starts at the deepest bound state accessible within the EFT. These discrete scaling symmetries are evident in Fig. 3. Similarly, it is possible to connect the scattering lengths at which the pole trajectory moves from the physical to the unphysical sheet by

$$a_-^{(n)} = \nu a_-^{(n+1)}. \tag{43}$$

Further, the symmetry manifests itself in a log-periodic behavior of the three-body observables. For convenience we introduce a dimensionless coupling $H(\Lambda) = D_0/\Lambda^4$. We renormalize $H(\Lambda)$ at $\gamma = 0$ such that the energy of the shallowest three-body bound state keeps fixed when varying the regulator scale Λ. This work uses two different renormalization prescriptions for $H(\Lambda)$. On the one hand, we choose a natural value for Λ and determine $H(\Lambda)$ to reproduce some three-body observable. On the other hand, we choose Λ such that $H(\Lambda) = 0$ [77].

The numerical procedure is as described above. Figure 4 shows a contour plot of the characteristic polynomial for an arbitrary scattering length along the contour. The resonance is identified by the zero in the fourth quadrant. Based on the Efimov structure of the pole trajectories, we present our results in units of a_-. Except for small Λ, where we cut off physically relevant momenta, or for large Λ, where our theory is no longer valid, all Efimov states are located on top of each other using this unit scheme.

This work is compared to the results by Bringas *et al.* [78] and Deltuva [79]. Similarly to this work, Bringas *et al.* use a Faddeev equation for a renormalized zero-range model and analytically continue it applying the rotation of the contour of integration. Deltuva solved the Faddeev equations for the transition operators for several short-range force models on the physical sheet and matched it to an expansion of the transition operator into a power series near the resonance pole. The derived pole trajectory is fitted by a lowest- and a higher-order approximation. The results of Bringas *et al.* and Deltuva are shown together with the pole trajectory derived within this work in Fig. 5. We only present one pole trajectory as both renormalization prescriptions result in indistinguishable trajectories. All results agree very well with our EFT calculation.

A further qualitative comparison is possible with the results by Jonsell [80], who investigates the three-boson system using a hyperspherical formalism together with the CSM, and with the work of Hyodo *et al.* [81], who calculate the pole trajectories using a contour rotation. The behavior of our pole trajectory is consistent with both these calculations.

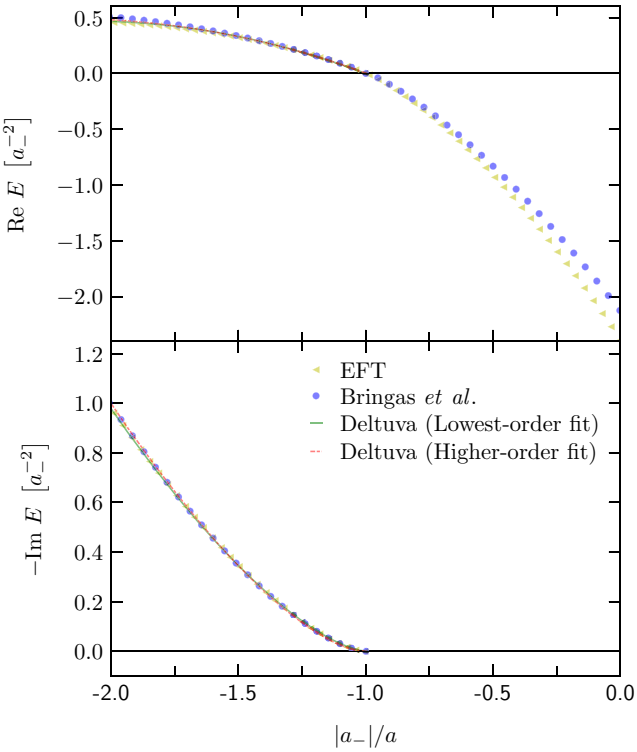

FIG. 5. Trajectories for the real (upper) and imaginary (lower) part of the three-boson pole energies. The trajectories are presented in units of a_- such that the transition from the physical to the unphysical sheet takes places at $|a_-|/a = -1$. The results derived in this work are compared to a calculation using the formalism by Bringas *et al.* [78] and two fits by Deltuva [79]. The latter ones are only present on the unphysical sheet. The pole trajectories presented here are equivalent to the trajectory sketched in Fig. 1 (dashed trajectory) as well as Fig. 3.

B. Three-neutron system

After benchmarking our method for the three-boson system, we focus on the three-neutron system. The easiest way to analytically continue the Faddeev equation would be to start with a bound-state pole on the physical sheet for an unphysical value of the *nn* scattering length as for the three-boson system. However, this method cannot be applied for the three-neutron system in leading-order pionless EFT because there is no three-body bound state for any value of the scattering length a.

This statement is based on the following argument: The structure of Eq. (34) in the limit $\Lambda \to \infty$ implies that if there is no three-body bound state for a particular value a of the neutron-neutron scattering length, then there is no bound state for any other value of a with the same sign. This argument relies on the fact that, for $\Lambda \to \infty$, a is the only dimensionful parameter in the equation and can be scaled out. The resulting dimensionless equation then applies for any finite value of a with the same sign. In the case of finite Λ, one can still exclude all physical bound states with energies well below the cutoff scale $|E| \ll \Lambda^2$. Finite range or other higher-order effects cannot change this conclusion as long as they are perturbative as stipulated by the power counting of pionless EFT. Based on this argument, we have excluded three-neutron bound states for $\lambda = 1$ and $\lambda = 0$.[5]

Since there are no bound states, we use a different ansatz. Glöckle used the same Faddeev equation for the degenerate channels $J^\pi = \frac{1}{2}^-$ and $J^\pi = \frac{3}{2}^-$, together with a Yamaguchi model $V_2(p,k) = -\kappa g(p) g(k)$, where

$$g(p) = \frac{1}{p^2 + \beta^2} \tag{44}$$

is a form factor [11]. Beside the interaction strength κ, this form factor implements a further scale β which induces a finite range. Using both parameters together it is possible to reproduce not only the scattering length, but also the effective range r_e which is included nonperturbatively. Keeping β fixed and increasing the interaction strength κ, this allows us to create a three-neutron bound state. Now, we are able to perform a calculation analogous to the three-boson system. Starting at a three-neutron bound state and reducing the two-neutron interaction strength κ while keeping β fixed (increasing the positive neutron-neutron scattering length) the pole trajectory moves through the two-body cut onto the unphysical sheet in the third quadrant of the complex energy plane. Decreasing κ further, the three- as well as the two-neutron poles finally arrive at zero. Following the pionless EFT power counting, we are able to reproduce this trajectory next to the origin for a going to infinity.

Figure 6 shows the part of this trajectory close to the origin together with LO EFT errors in comparison to the results derived using the Yamaguchi model. Along both trajectories the values of the scattering length (in fm) for selected points are indicated.

Now, we arrive at the interesting part of the pole trajectory: an unbound two-neutron subsystem. Within Ref. [11], the pole trajectory continues on an unphysical sheet which is different from the relevant unphysical sheet next to the lower rim of the physical sheet. So, the pole at the physical set of parameters is too far away from the physical sheet and has no effect on observables.

To see if this is different using the Gaussian regulator, we follow the explanation above and investigate the absolute value of the determinant of $\mathbb{1}$ minus the kernel of Eq. (40) in the complex momentum plane. A zero within this plot would indicate a possible pole. This investigation is performed for negative values of a starting at 0 fm up to the physical value $a \approx -18.9$ fm. Figure 7 shows an example of what these contour plots look like. Beside the expected discretized cut structures resulting from the structure of the equation, no behavior that can be connected to a pole is visible. So, using a Gaussian regulator we recover the results of Ref. [11]. This outcome is also supported by the power counting, predicting that we should be able to recover the results of the Yamaguchi type regulator for large negative scattering lengths.

Similarly to the negative parity channels discussed above, we have investigated the analytically continued Faddeev

[5]Higher values of λ were not considered explicitly, but we do not expect any bound states there, either.

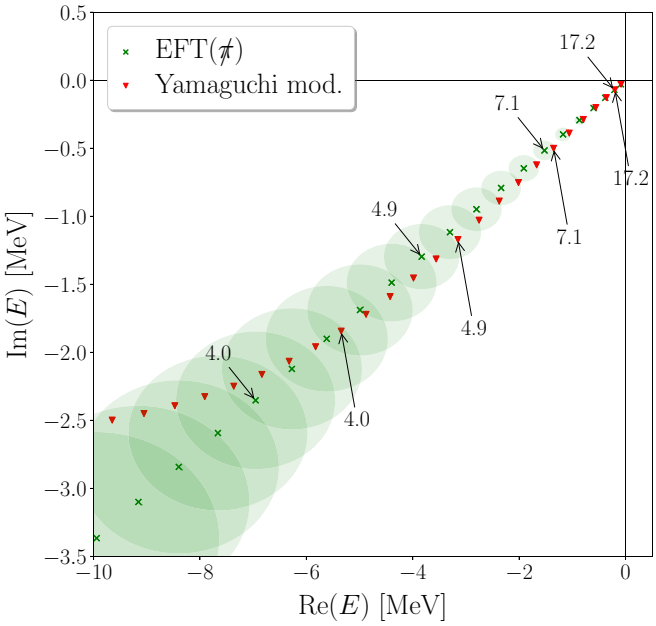

FIG. 6. The pole trajectory of the three-neutron system ($J^\pi = \frac{1}{2}^-$ and $J^\pi = \frac{3}{2}^-$) for positive scattering length for a pionless EFT interaction together with the LO error bands in comparison to a calculation using the Yamaguchi model. The values of the scattering length in fm for selected points are given by the numbers and arrows. The pole trajectory calculated using the Yamaguchi model is equivalent to the trajectory sketched in Fig. 1 (solid trajectory). While the pionless EFT calculation only includes the scattering length, the Yamaguchi model incorporates higher order effective range effects. The results are presented in the complex energy plane. The lower half-plane shows the unphysical sheet accessed through the two-body cut. Within the region where EFT(/) is valid, both trajectories agree within the EFT error indicated by the LO circles.

equation for the $J^\pi = \frac{1}{2}^+$ channel ($\lambda = 0$) in the complex momentum plane in the vicinity of the physical nn scattering length. We found no evidence of a three-neutron resonance in the $J^\pi = \frac{1}{2}^+$ channel, either.

V. FINITE VOLUME

Finite-volume calculations were established in Ref. [63] as a tool to identify few-body resonance states. This approach goes back to the pioneering work of Lüscher [65,66], who first showed that properties of the infinite-volume S matrix, and therefore observables like bound states and scattering parameters, are encoded in how the discrete energy levels in a finite periodic box change as the size L of the box is varied. Resonance states are manifest as avoided crossings of energy levels, which is well established for two-body systems [59–61] and routinely used to extract resonance properties from lattice QCD calculations [82]. In Ref. [63], it was demonstrated that this signature carries over to the few-body sector. We use here these findings, and in particular the discrete variable representation (DVR), as an additional, independent tool to search for three-neutron resonances.

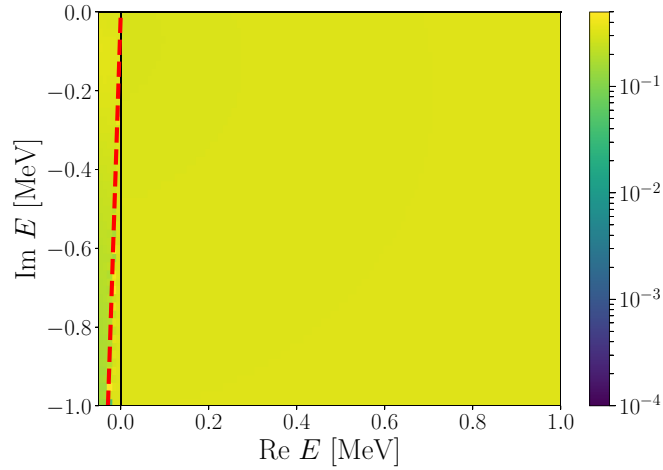

FIG. 7. A contour plot presenting the absolute value of the determinant of one minus the kernel of Eq. (40) on the unphysical sheet adjacent the three-body cut. This calculation was performed for $a = -18.77$ fm and a rotation angle $\varphi = 0.8$ rad. Similarly to Fig. 4, the three-body cut is visible at an angle $2\varphi = 1.6$ rad (91.67°) next to the negative imaginary axis. A zero within this plot is equivalent to an eigenvalue equal to 1 of Eq. (40), which itself corresponds to a possible physical state. So, this plot presents no evidence for a possible three-neutron resonance in the degenerate $J^\pi = \frac{1}{2}^-$ and $J^\pi = \frac{3}{2}^-$ channels.

A. Basic setup

The starting point for the DVR construction of states in a periodic box with edge length L are plane-wave states $\phi_j(x)$ with $j = -n/2, \ldots, n/2 - 1$ for even $n > 2$, where x denotes the relative coordinate describing a two-body ($N = 2$) system in one dimension ($d = 1$). Any periodic solution of the one-dimensional (1D) Schrödinger equation can be expanded in terms of the states $\phi_j(x)$, yielding a discrete Fourier transform (DFT). Given a set of equidistant points $x_k \in [-L/2, L/2)$ and weights $w_k = L/n$ (independent of k), DVR states are constructed as [83]

$$\psi_k(x) = \sum_{i=-n/2}^{n/2-1} \mathcal{U}^*_{ki} \phi_i(x), \tag{45}$$

with $\mathcal{U}_{ki} = \sqrt{w_k}\phi_i(x_k)$ defining a unitary matrix. The DVR is convenient for two main reasons:

(1) For a local interaction, the potential operator V reduces (approximately) to a diagonal matrix, $\langle\psi_k|V|\psi_l\rangle \approx V(x_k)\delta_{kl}$, where the quality of this approximation is determined by the number n of discretization points. This holds for any number d of spatial dimensions and N interacting particles.

(2) The kinetic energy K is *not* diagonal, but its form is known analytically:

$$\langle\psi_k|K|\psi_l\rangle = \begin{cases} \frac{\pi^2 N^2}{6\mu L^2}\left(1 + \frac{2}{n^2}\right) & \text{for } k = l, \\ \frac{(-1)^{k-l}\pi^2}{\mu L^2 \sin^2[\pi(k-l)/n]} & \text{otherwise.} \end{cases} \tag{46}$$

For $d > 1$ or $N > 2$ the DVR representation of K becomes a sparse matrix that can be calculated very efficiently based only on the $d = 1$, $N = 2$ elements. Alternatively, as pointed out in Ref. [84], one can exploit the relation of the plane-wave based DVR to the DFT and evaluate the kinetic energy in momentum space, but we find the direct calculation more efficient for large-scale calculations.

The construction is straightforward to generalize to the case of an arbitrary number of particles N and spatial dimensions d, starting from product states of $(N-1)\times d$ plane waves, one for each relative-coordinate component. The transformation matrices and DVR basis functions are defined via tensor products, and DVR states are labeled by a collection of $(N-1)\times d$ indices. Using the shorthand notation $|\psi_k\rangle = |k\rangle$, a general state is written as

$$|s\rangle = |(k_{1,1},\ldots,k_{1,d}),\ldots,(k_{N-1,1},\ldots,k_{N-1,d});(\sigma_1,\ldots,\sigma_N)\rangle, \tag{47}$$

where the σ_i denote the spin degrees of freedom. The space spanned by all these states $|s\rangle$ is denoted by B. For spinless bosons, $\sigma_i = 0$ for all i, whereas in general, for particles with spin S, $\sigma_i = -S,\ldots,S$. Specifically, we have here $S = 1/2$, $d = 3$, and $N = 3$ for the three-neutron system we study.

Fore more details regarding the DVR setup we refer to Refs. [63,85] and further references cited therein, and merely recall here that the overall strategy with this method is to represent the N-body finite-volume Hamiltonian $H = H_0 + V$, where $H_0 = \hat{K}$ is the relative kinetic energy operator and V denotes the sum of all interactions among the particles, as a matrix in the space spanned by the DVR states. Energy levels in the box are then obtained by calculating the spectrum (or more specifically the lowest lying states in the spectrum) via Lanczos/Arnoldi iteration.

B. Separable interactions

The DVR as described above is set up only to work with local potentials. In order to study in finite volume the same separable potentials as used for the momentum-space calculation, we discuss in the following the appropriate extension of the DVR formalism. We start from the definition of a general DVR state, Eq. (47), and neglect for the moment the spin degrees of freedom.

Recall that projected onto coordinate space a state $|s\rangle$ is a product of one-dimensional DVR wave functions,

$$\psi_s(\underline{x}) = \langle \underline{x}|s\rangle = \prod_{\substack{i=1,\ldots,N-1\\ c=1,\ldots,d}} \psi_{k_{i,c}}(x_{i,c}), \tag{48}$$

where $\underline{x}$ is used to denote the collection of all relative coordinates. Furthermore, let $\psi(\underline{x})$ be a generic state expanded in the DVR basis B,

$$\psi(\underline{x}) = \sum_{s\in B} c_s \psi_s(\underline{x}). \tag{49}$$

This could be an actual eigenstate of the Hamiltonian, or any intermediate state vector that is encountered during the Lanczos-based diagonalization of the Hamiltonian. Either way, the $\{c_s\}$ is a finite vector of coefficients with entries as introduced in Eq. (47).

Let us now consider a (rank-1) separable two-body potential, generically written in coordinate space as

$$V_2(x,x') = C\, g(x) g(x'), \tag{50}$$

where C is the strength and $|g\rangle$ with $\langle x|g\rangle = g(x)$ is the "form factor." For simplicity we restrict the following discussion to one spatial dimension since everything carries over to $d > 1$ in a straightforward way. For a two-body state, we have $\underline{x} = x_1 \equiv x$ and $|s\rangle = |k\rangle$ (a single index describes the spinless 1D state), so that applying V is straightforward:

$$\begin{aligned}\langle s|V_2|\psi\rangle &= \int dx \int dx'\, \psi_s^*(x') V_2(x,x') \sum_{s'\in B} c_{s'}\psi_{s'}(x') \\ &= C\, g(x_s) \sum_{s'\in B} c_{s'}\, g(x_{s'}).\end{aligned} \tag{51}$$

We have used here the DVR property of the states, and $x_s = x_k$ is the location of the lattice point characterizing the state $|s\rangle$. It follows that, for this case, applying a separable potential to a generic DVR state is very simple, and the factorization property of the potential is directly reflected in the end result.

For more than two particles one (in general) needs to consider the separable potential (50) between all pairs of particles. Since for each pairwise interaction the potential only involves the relative coordinate of that pair, appropriate delta functions need to be included for all "spectator" particles that do not take part in the particular interaction. The way to do this consistently across all pairs is to express these delta functions such that they fix the position of the spectators relative to the center of mass of the interacting pair (which amounts to a partial transformation to a particular set of Jacobi coordinates, similar to what is used in the Faddeev formalism discussed in the main text).

A minor complication arises from the fact that in a periodic finite volume the center of mass of a cluster of particles is not uniquely defined. This can already be seen for two particles in one dimension: consider these particles on a periodic interval from 0 to L residing at positions $x = 1$ and $x = L-1$; then both $x = 0$ and $x = L/2$ are valid candidates for the particle's center of mass. Visualizing the periodic interval as a circle, these two possibilities correspond to the middle points of the two arcs that connect the particles. With increasing number of dimensions and number of particles, the set of candidates for the center of mass becomes larger. Which one is chosen is arbitrary, but the choice has to be consistent. To that end, for a configuration of A coordinates $C = \{\mathbf{x}_i\}_{i=1}^A$ we define the center of mass to be that point that minimizes the sum of distances of all particles measured with respect to the center of mass:

$$\mathbf{R}_{\rm cm} = \underset{\mathbf{R}\in S_{\rm cm}(C)}{\arg\min}\left(\sum_{j=1}^{A} d_L(\mathbf{R},\mathbf{x}_j)^2\right), \tag{52}$$

where $S_{\rm cm}(C)$ is the set of all possible center-of-mass coordinates for the given configuration C and d_L measures the distance between two points as the shortest path between them while accounting for the periodic boundary condition.

Taking into account the spatial lattice nature of the plane-wave DVR basis and noting that for an A-body state on a lattice of extent n the center of mass falls onto a lattice with extent nA [86], it becomes straightforward to express the center-of-mass coordinate as an index in an enlarged DVR space. For each given pair interaction V_{ij}, denoting a potential of the form (50) acting between particles i and j, such an index is considered for each spectator particle in order to include appropriate Kronecker deltas. Schematically, Eq. (51) becomes

$$\langle s|V_{ij}|\psi\rangle = \mathcal{N} \times C\, g(x_{s;ij}) \sum_{\substack{s'\in B \\ r_{s';k,ij}=r_{s;k,ij}\forall k\neq i,j}} c_{s'}\, g(x_{s';ij}). \tag{53}$$

Here $x_{s;ij}$ denotes the relative distance (modulo the periodic boundary) between particles i and j in configuration $|s\rangle$ and $r_{s;k,ij}$ is the coordinate of particle k relative to the center of mass of particles i and j as defined in Eq. (52), for $A = 2$. The generalization to $d > 1$ is trivial, and only a minor technical complication arises from the fact that the DVR states are expressed in relative coordinates. For $j = N$ one can directly work with the x_i (or $x_{i,c}$ in $d > 1$), whereas for other pairs one considers appropriate differences of the x_i that give the desired coordinate vector. The factor $\mathcal{N} = 2^d(L/N)^{d/2}$ arises as normalization from the integral over spectator coordinates.

Since the plane-wave DVR states we consider are closely related to a DFT [84,85], this is naturally the tool to use for calculating matrix elements $\langle s|V_{ij}|\psi\rangle$ when the V_{ij} are given in momentum space. To that end, one considers two-body momentum modes

$$p_j = \frac{2\pi j}{L} \tag{54}$$

and, for the appropriate coordinate $x_{s;ij}$ as introduced above, evaluates

$$\langle s|g\rangle = \sum_{k=-n/2}^{n/2} g(p_k)\, \exp(ip_k x_{s;ij}). \tag{55}$$

This equation is written for the one-dimensional case, but it straightforwardly generalizes to $d > 1$. The considerations about including appropriate delta functions to fix the coordinates of the spectator particles relative to the interacting pair's center of mass remain exactly the same and need not be carried out in momentum space.

The momentum-space implementation also makes it particularly convenient to consider interactions that act only in a single partial wave. The following considerations can easily be generalized to arbitrary d, but we consider here only the most relevant case $d = 3$. For spinless particles, the projection is achieved by merely including a factor $|\mathbf{p_k}|^l Y_{lm}(\hat{\mathbf{p}}_\mathbf{k})$ in the three-dimensional generalization of Eq. (55), where $\mathbf{p_k}$ is a momentum mode in 3D and Y_{lm} denotes the spherical harmonic for angular momentum l and projection m.[6] Note that since the DVR uses a full three-dimensional model space (not decomposed into partial waves), a potential term needs to be included for each $m = -l, \ldots, l$. To include spin, one can directly utilize the projection indices σ_k included in the states (47). If the interaction is meant to act in a two-body channel $^{2s+1}l_j$, written in spectroscopic notation, one includes a Clebsch-Gordan coefficient that couples the individual particles spins to s (where the total projection is fixed to be $\sigma_i + \sigma_j$), and then another Clebsch-Gordan coefficient that couples l and s to total angular momentum j. For this case, one has a potential for each $m_j = -j, \ldots, j$, and all projection quantum numbers in the Clebsch-Gordan coefficients are fully determined by this, the spin projection, and the standard Clebsch-Gordan selection rules. This means that there are no extra sums required to carry out the partial-wave projection. In essence, this sum is the one appearing already in Eq. (53).

For practical implementations it is desirable to avoid complex arithmetic as much as possible. To achieve that, it is convenient to work with real spherical harmonics instead of the Y_{lm} and replace in Eq. (55) the exponential function with a cosine or sine for even and odd l, respectively.

C. Results

For EFT applications it is convenient to express the separable potential (50) in momentum space as

$$V_2(q, q') = C\, g(q)g(q'), \tag{56}$$

where $g(q)$ is the Fourier transform of $g(r)$, indicated only by the argument for simplicity. In typical applications the potential is often given directly in the form (56). We pick here specifically a super-Gaussian form:

$$g(q) = \exp(-q^{2n}/\Lambda^{2n}). \tag{57}$$

The Faddeev calculations discussed in Sec. II use this form with $n = 1$. To ensure that our finite-volume implementation of separable interactions is correct, we have run bound-state benchmark calculations with such simple Gaussian form factors for some selected potentials. For the three-neutron results discussed in the following, however, we chose to work with $n = 2$ because this regulator form provides a stronger suppression of high-momentum modes, which helps to achieve converged calculations in large boxes. We moreover chose a rather soft cutoff scale $\Lambda = 250$ MeV for these calculations.

Results are shown in Figs. 8–10 for total spin $S = 1/2$ and negative parity. A projection on the representations of the cubic symmetry group of the box shows that these energy levels correspond to the degenerate $J^\pi = \frac{1}{2}^-$ and $J^\pi = \frac{3}{2}^-$ channels we are primarily interested in. We start with the physical neutron-neutron scattering length (Fig. 8) and then gradually adjust the interaction to become more attractive. In particular, for $a = +18.9$ fm (Fig. 9) and $a = +10.0$ fm (Fig. 10) the interaction supports shallow dineutron bound states with energy $E_2 = 1/(M_n a^2)$. In the three-body spectrum we can see the effect of the increasing attraction directly reflected in the fact that all energy levels get shifted downwards in going from Figs. 8 to 10. The comparison of different DVR basis size (solid and dashed lines in the figures) shows that we can achieve sufficiently converged calculations in the energy range where three-neutron resonances have been speculated to

[6]Note that $|\mathbf{p_k}|^l Y_{lm}(\hat{\mathbf{p}}_\mathbf{k})$ really is a solid harmonic in momentum space.

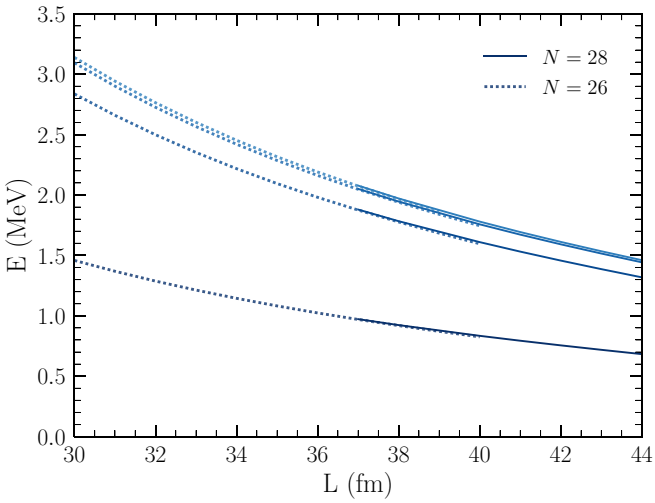

FIG. 8. Finite-volume energy levels for three neutrons with total spin $S = 1/2$ and negative parity, calculated assuming a separable $n = 2$ super-Gaussian interaction tuned to reproduce a neutron-neutron scattering length $a = -18.9$ fm. The solid (dashed) lines were obtained using $N = 26$ (28) mesh points to construct the three-neutron DVR basis.

exist. However, for the values of the scattering length considered, we do not see avoided level crossings in the spectrum or plateau shapes in individual energy levels. Thus, we see none of the signatures of a resonance discussed in Ref. [63]. Our finite-volume results thus confirm the findings of our Faddeev calculations that there are no resonances in the degenerate $J^\pi = \frac{1}{2}^-$ and $J^\pi = \frac{3}{2}^-$ channels, and we conclude that even with increased attraction in the neutron-neutron S-wave interaction there is no support for a three-neutron resonance state in the most likely channel. For the physical neutron-neutron scattering length we have furthermore calculated a positive-parity spectrum (not shown as an explicit figure), in which we see no indications for a three-neutron resonance either.

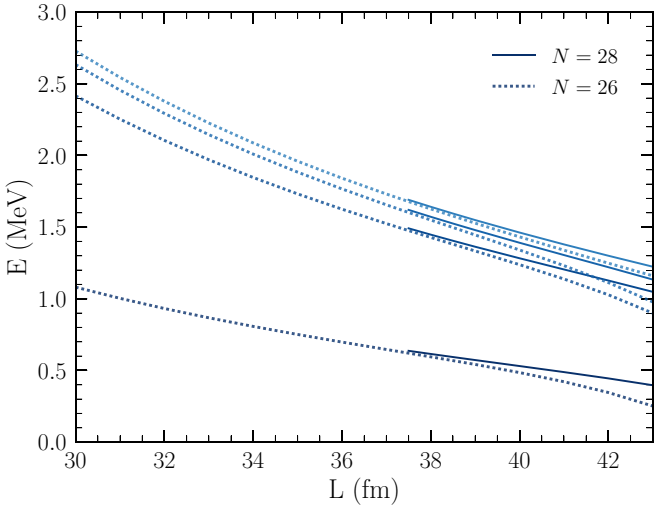

FIG. 9. Same as Fig. 8, except with the interaction tuned to a neutron-neutron scattering length $a = +18.9$ fm.

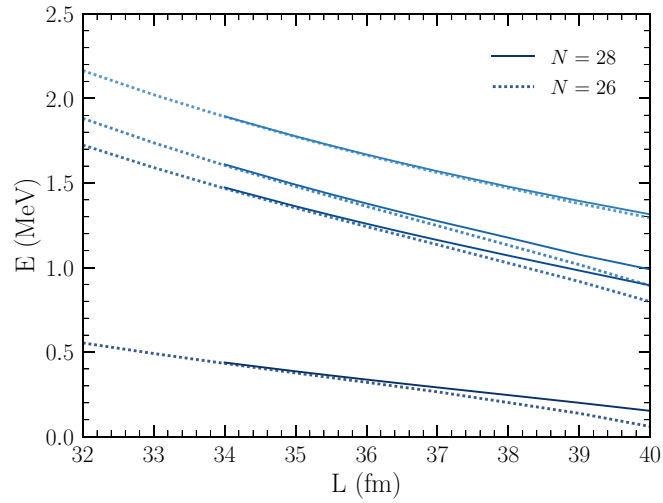

FIG. 10. Same as Fig. 8, except with the interaction tuned to a neutron-neutron scattering length $a = +10.0$ fm.

VI. CONCLUSION AND OUTLOOK

In this work, we have presented a rigorous study of the appearance of resonances in three-body systems using two complementary methods. We first use pionless effective field theory at leading order to write down an effective interaction potential which may include a three-body interaction. In the second step, we analytically continue the Faddeev equation in momentum space to the unphysical sheet adjacent to the positive real energy axis using a rotation of the integration contour. On the unphysical sheet, we search for poles corresponding to resonances and virtual states. This direct search for resonance poles is complemented by an alternative finite-volume method based on identifying avoided crossings of energy levels as the size of the volume is varied. The two methods have very different systematics and ideally complement each other, although the latter method is not suitable for virtual states.

We apply our framework to two types of systems: (i) three bosons with large negative scattering length a and (ii) the three-neutron system. Our study of the three-boson system also serves as a test case of our method. It is well known that three-body Efimov states for $a < 0$ turn into resonances as they cross the three-particle threshold. We confirm the previous calculations by Bringas *et al.* [78] and Deltuva [79] both qualitatively and quantitatively. Moreover, our results are qualitatively consistent with the pole trajectories of Jonsell [80] and Hyodo *et al.* [81]. The trajectories of the Efimov resonances can be used to explain the behavior of the three-body recombination rate of three spinless bosons at low temperatures [80,87].

The main motivation for our work is the suggestion of a low-energy resonance or virtual state in the three-neutron system [3,7]. We can reproduce earlier calculations by Glöckle for a three-neutron Yamaguchi model system with a strong attraction [11]. However, we do not find any resonances for the physical case in the relevant $\lambda = 1$ and $\lambda = 0$ orbital angular momentum channels corresponding to the $J^\pi = \frac{1}{2}^-$, $\frac{3}{2}^-$, and $\frac{1}{2}^+$ channels in the analytical continuation framework. Low-

energy resonances in the negative parity channels are also excluded in the finite-volume framework. Using the analytical continuation method, we also exclude a three-neutron virtual state. Our model-independent result agrees with several other recent theoretical studies [5,8–10] and rules out the possibility of a three-neutron resonance or virtual state at low energy. Although we use pionless EFT at leading order, we expect our result to hold also in the presence of higher-order interactions. In pionless EFT the higher-order terms, including the effective range r_0 and P-wave interactions, are purely perturbative and cannot produce any new poles. Thus the existence of a low-energy three-neutron resonance would also imply the breakdown of pionless EFT in the three-neutron system.

Obviously, our study does not address the question of four-neutron resonances. Experimental evidence for such a four-neutron resonance was recently presented in [23]; see also Ref. [28] for a current review of the field. We leave this question for future work.

Finally, we stress that multineutron energy spectra contain much interesting physics, even if multineutron resonances are not observed in experiment. In Ref. [88], e.g., it was pointed out that the multineutron spectra for center-of-mass energies E in the range $1/(ma^2) \approx 0.1\,\text{MeV} \ll E \ll 1/(mr_0^2) \approx 5\,\text{MeV}$ are determined by conformal symmetry up an overall normalization. Conformal symmetry implies that the multineutron correlation functions have only cuts but no poles, which is consistent with our results for the three-neutron system. The neutron spectra show power-law behavior with, in general, fractional exponents determined by the scaling dimension of the corresponding conformal field operators. This is markedly different from weakly interacting particles. Neutron resonance experiments are ideally suited to confirm this prediction.

ACKNOWLEDGMENTS

We thank Joel Lynn for collaboration in the early stages of this work, and Dean Lee for useful discussions regarding the implementation of separable interactions in finite volume. This work was supported in part by the Deutsche Forschungsgemeinschaft (DFG, German Research Foundation), Project-ID 279384907, SFB 1245, by the BMBF Contracts No. 05P18RDFN1 and No. 05P21RDFNB, and by the National Science Foundation under Grant No. PHY–2044632. This material is based upon work supported by the U.S. Department of Energy, Office of Science, Office of Nuclear Physics, under the FRIB Theory Alliance Award No. DE-SC0013617. Computational resources for parts of this work were provided by the Jülich Supercomputing Center.

[1] I. Slaus, in *Few Particle Problems: Proceedings of the International Conference on Few Particle Problems in the Nuclear Interaction*, Los Angeles, August 28–September 1, 1972 (Elsevier Science, Burlington, 1972), pp. 539–542.

[2] R. Y. Kezerashvili, Search of Trineutron and Tetraneutron, in *6th International Conference on Fission and Properties of Neutron Rich Nuclei* (World Scientific, Singapre, 2016).

[3] S. Gandolfi, H. W. Hammer, P. Klos, J. E. Lynn, and A. Schwenk, Is a Trineutron Resonance Lower in Energy than a Tetraneutron Resonance? Phys. Rev. Lett. **118**, 232501 (2017).

[4] P. Truöl and J. Miller, Comment on arXiv:1612.01502 'Is the Trineutron Resonance Lower in Energy than a Tetraneutron Resonance?' arXiv:1708.04459.

[5] A. Deltuva, Three-neutron resonance study using transition operators, Phys. Rev. C **97**, 034001 (2018).

[6] A. Deltuva and R. Lazauskas, Comment on "Is a Trineutron Resonance Lower in Energy than a Tetraneutron Resonance?", Phys. Rev. Lett. **123**, 069201 (2019).

[7] J. G. Li, N. Michel, B. S. Hu, W. Zuo, and F. R. Xu, *Ab initio* no-core Gamow shell-model calculations of multineutron systems, Phys. Rev. C **100**, 054313 (2019).

[8] S. Ishikawa, Three-neutron bound and continuum states, Phys. Rev. C **102**, 034002 (2020).

[9] M. D. Higgins, C. H. Greene, A. Kievsky, and M. Viviani, Nonresonant Density of States Enhancement at Low Energies for Three or Four Neutrons, Phys. Rev. Lett. **125**, 052501 (2020).

[10] M. D. Higgins, C. H. Greene, A. Kievsky, and M. Viviani, Comprehensive study of the three- and four-neutron systems at low energies, Phys. Rev. C **103**, 024004 (2021).

[11] W. Glöckle, S-matrix pole trajectory in a three-neutron model, Phys. Rev. C **18**, 564 (1978).

[12] K. Möller, Untersuchung von Resonanzen in Dreinukleonensystemen, Ph.D. thesis, Zentralinstitut für Kernforschung, Dresden, 1979.

[13] J. P. Miller, J. A. Bistirlich, K. M. Crowe, S. S. Rosenblum, P. C. Rowe, F. T. Shively, E. R. Grilly, E. C. Kerr, J. Novak, R. H. Sherman *et al.*, Upper limits for bound states and resonance behavior in the trineutron system, Nucl. Phys. A **343**, 347 (1980).

[14] A. Stetz, L. W. Swenson, J. Davis, J. Kallne, R. C. Minehart, R. R. Whitney, V. Perez-Mendez, A. Sagle, J. Carroll, J. B. McClelland *et al.*, Pion double charge exchange on ^{3}He and ^{4}He, Nucl. Phys. A **457**, 669 (1986).

[15] D. R. Tilley, H. R. Weller, and H. H. Hasan, Energy levels of light nuclei $A = 3$, Nucl. Phys. A **474**, 1 (1987).

[16] M. Yuly, W. Fong, E. R. Kinney, C. J. Maher, J. L. Matthews, T. Soos, J. Vail, M. Y. Wang, S. A. Wood, P. A. M. Gram, G. A. Rebka, and D. A. Roberts, Pion double charge exchange and inelastic scattering on ^{3}He, Phys. Rev. C **55**, 1848 (1997).

[17] R. Offermann and W. Glöckle, Is there a three-neutron resonance? Nucl. Phys. A **318**, 138 (1979).

[18] S. A. Sofianos, S. A. Rakityansky, and G. P. Vermaak, Subthreshold resonances in few neutron systems, J. Phys. G **23**, 1619 (1997).

[19] A. Csoto, H. Oberhummer, and R. Pichler, Searching for three nucleon resonances, Phys. Rev. C **53**, 1589 (1996).

[20] H. Witała and W. Glöckle, Resonances in the three neutron system, Phys. Rev. C **60**, 024002 (1999).

[21] A. Hemmdan, W. Glöckle, and H. Kamada, Indications for the nonexistence of three neutron resonances near the physical region, Phys. Rev. C **66**, 054001 (2002).

[22] R. Lazauskas and J. Carbonell, Three-neutron resonance trajectories for realistic interaction models, Phys. Rev. C **71**, 044004 (2005).

[23] K. Kisamori, S. Shimoura, H. Miya, S. Michimasa, S. Ota, M. Assie, H. Baba, T. Baba, D. Beaumel, M. Dozono *et al.*, Candidate Resonant Tetraneutron State Populated by the ^{4}He(^{8}He, ^{8}Be) Reaction, Phys. Rev. Lett. **116**, 052501 (2016).

[24] T. Faestermann, A. Bergmaier, R. Gernhäuser, D. Koll, and M. Mahgoub, Indications for a bound tetraneutron, Phys. Lett. B **824**, 136799 (2022).

[25] S. Gandolfi, H.-W. Hammer, P. Klos, J. E. Lynn, and A. Schwenk, Reply to 'Comment on "Is a Trineutron Resonance Lower in Energy than a Tetraneutron Resonance?"' Phys. Rev. Lett. **123**, 069202 (2019).

[26] A. Deltuva, M. Gattobigio, A. Kievsky, and M. Viviani, Gaussian characterization of the unitary window for $n = 3$: Bound, scattering, and virtual states, Phys. Rev. C **102**, 064001 (2020).

[27] R. Schiavilla, L. Girlanda, A. Gnech, A. Kievsky, A. Lovato, L. E. Marcucci, M. Piarulli, and M. Viviani, Two- and three-nucleon contact interactions and ground-state energies of light- and medium-mass nuclei, Phys. Rev. C **103**, 054003 (2021).

[28] F. M. Marqués and J. Carbonell, The quest for light multineutron systems, Eur. Phys. J. A **57**, 105 (2021).

[29] U. van Kolck, Nucleon-nucleon interaction and isospin violation, in *Chiral Dynamics: Theory and Experiment*, Lecture Notes in Physics Vol. 513 (Springer, Berlin, 1998).

[30] D. B. Kaplan, M. J. Savage, and M. B. Wise, A new expansion for nucleon-nucleon interactions, Phys. Lett. B **424**, 390 (1998).

[31] D. B. Kaplan, M. J. Savage, and M. B. Wise, Two nucleon systems from effective field theory, Nucl. Phys. B **534**, 329 (1998).

[32] U. van Kolck, Effective field theory of short range forces, Nucl. Phys. A **645**, 273 (1999).

[33] E. Braaten and H. W. Hammer, Universality in few-body systems with large scattering length, Phys. Rep. **428**, 259 (2006).

[34] P. Naidon and S. Endo, Efimov physics: a review, Rep. Prog. Phys. **80**, 056001 (2017).

[35] S. R. Beane, P. F. Bedaque, W. C. Haxton, D. R. Phillips, and M. J. Savage, From hadrons to nuclei: Crossing the border, in *At the Frontier of Particle Physics—Handbook of QCD* (World Scientific, Singapore, 2000), pp. 133–271.

[36] P. F. Bedaque and U. van Kolck, Effective field theory for few-nucleon systems, Annu. Rev. Nucl. Part. Sci. **52**, 339 (2002).

[37] E. Epelbaum, H.-W. Hammer, and Ulf-G. Meißner, Modern Theory of Nuclear Forces, Rev. Mod. Phys. **81**, 1773 (2009).

[38] H.-W. Hammer, S. König, and U. van Kolck, Nuclear effective field theory: Status and perspectives, Rev. Mod. Phys. **92**, 025004 (2020).

[39] A. Schwenk and C. J. Pethick, Resonant Fermi Gases with a Large Effective Range, Phys. Rev. Lett. **95**, 160401 (2005).

[40] L. D. Faddeev, Scattering theory for a three-particle system, Sov. Phys. JETP **12**, 1014 (1961).

[41] C. Lovelace, in *Strong Interactions and High Energy Physics*, edited by R. G. Moorhouse (Oliver and Boyd, London, 1964).

[42] K. Möller, Investigation of Resonances in the ^{3}n-System, in *Proceedings of the 1977 European Symposium on Few Particle Probl. in Nucl. Phys., Potsdam, Oct. 11–14, 1977*, Report No. ZFK-347, German Democratic Republic, 1977, p. 90.

[43] K. Möller, On a method for calculating the eigenvalues of the Faddeev Equation Kernel on the Nonphysical Sheet of Energy, Report No. ZFK-327, German Democratic Republic, 1977.

[44] K. Möller, On the calculation of the eigenvalues of the Faddeev equation kernel on the nonphysical sheet of energy, Report No. ZFK-351, German Democratic Republic, 1978.

[45] K. Möller, S Matrix Pole Trajectories of the Efimov States, Report No. ZFK-357, German Democratic Republic, 1978.

[46] K. Möller, Determination of the dominant resonance pole of the three-neutron system, Report No. ZFK-437, German Democratic Republic, 1981.

[47] B. C. Pearce and I. R. Afnan, Resonance poles in three-body systems, Phys. Rev. C **30**, 2022 (1984).

[48] I. R. Afnan, Resonances in few body systems, Aust. J. Phys. **44**, 201 (1991).

[49] I. R. Afnan and B. F. Gibson, Resonances in Λd scattering and the Σ hypertriton, Phys. Rev. C **47**, 1000 (1993).

[50] I. R. Afnan and B. F. Gibson, Resonances in the Λnn system, Phys. Rev. C **92**, 054608 (2015).

[51] B. Gibson and I. Afnan, The Λn scattering length and the Λnn resonance, in *The 13th International Conference on Hypernuclear and Strange Particle Physics: HYP2018*, 24–29 June 2018, Virginia, edited by L. Tang and R. Schumacher, AIP Conf. Proc. No. 2130 (AIP, New York, 2019), p. 020005.

[52] J. Aguilar and J. M. Combes, A class of analytic perturbations for one-body Schrödinger Hamiltonians, Commun. Math. Phys. **22**, 269 (1971).

[53] E. Balslev and J. M. Combes, Spectral properties of many-body Schrödinger operators with dilatation-analytic interactions, Commun. Math. Phys. **22**, 280 (1971).

[54] T. Myo, Y. Kikuchi, H. Masui, and K. Katō, Recent development of complex scaling method for many-body resonances and continua in light nuclei, Prog. Part. Nucl. Phys. **79**, 1 (2014).

[55] T. Myo and K. Kato, Complex scaling: Physics of unbound light nuclei and perspective, Prog. Theor. Exp. Phys. **2020**, 12A101 (2020).

[56] R. Lazauskas, Application of the complex scaling method in quantum scattering theory, Habilitation thesis, 2019 (unpublished), arXiv:1904.04675.

[57] T. Berggren, On the use of resonant states in eigenfunction expansions of scattering and reaction amplitudes, Nucl. Phys. A **109**, 265 (1968).

[58] T. Berggren and P. Lind, Resonant state expansion of the resolvent, Phys. Rev. C **47**, 768 (1993).

[59] U. J. Wiese, Identification of Resonance Parameters From the Finite Volume Energy Spectrum, in *LATTICE 88, Proceedings*, Batavia, NY, September 22–25, 1988 [Nucl. Phys. B Proc. Suppl. **9**, 609 (1989)].

[60] M. Lüscher, Signatures of unstable particles in finite volume, Nucl. Phys. B **364**, 237 (1991).

[61] K. Rummukainen and S. A. Gottlieb, Resonance scattering phase shifts on a non-rest-frame lattice, Nucl. Phys. B **450**, 397 (1995).

[62] P. Klos, J. E. Lynn, I. Tews, S. Gandolfi, A. Gezerlis, H. W. Hammer, M. Hoferichter, and A. Schwenk, Quantum Monte Carlo calculations of two neutrons in finite volume, Phys. Rev. C **94**, 054005 (2016).

[63] P. Klos, S. König, H.-W. Hammer, J. E. Lynn, and A. Schwenk, Signatures of few-body resonances in finite volume, Phys. Rev. C **98**, 034004 (2018).

[64] M. Lüscher, Volume Dependence of the energy spectrum in massive quantum field theories. 1. Stable particle states, Commun. Math. Phys. **104**, 177 (1986).

[65] M. Lüscher, Volume dependence of the energy spectrum in massive quantum field theories. 2. Scattering states, Commun. Math. Phys. **105**, 153 (1986).
[66] M. Lüscher, Two particle states on a torus and their relation to the scattering matrix, Nucl. Phys. B **354**, 531 (1991).
[67] L. Platter, H.-W. Hammer, and Ulf-G. Meißner, The Four boson system with short range interactions, Phys. Rev. A **70**, 052101 (2004).
[68] L. Platter, H.-W. Hammer, and U.-G. Meißner, On the correlation between the binding energies of the triton and the alpha-particle, Phys. Lett. B **607**, 254 (2005).
[69] P. F. Bedaque and U. van Kolck, Nucleon deuteron scattering from an effective field theory, Phys. Lett. B **428**, 221 (1998).
[70] P. F. Bedaque, H.-W. Hammer, and U. van Kolck, Effective theory for neutron deuteron scattering: Energy dependence, Phys. Rev. C **58**, R641 (1998).
[71] P. F. Bedaque, H.-W. Hammer, and U. van Kolck, Renormalization of the Three-Body System with Short-Range Interactions, Phys. Rev. Lett. **82**, 463 (1999).
[72] P. F. Bedaque, H.-W. Hammer, and U. van Kolck, The Three boson system with short range interactions, Nucl. Phys. A **646**, 444 (1999).
[73] A. Gardestig, Extracting the neutron-neutron scattering length—recent developments, J. Phys. G **36**, 053001 (2009).
[74] A. Stadler, W. Glöckle, and P. U. Sauer, Faddeev equations with three-nucleon force in momentum space, Phys. Rev. C **44**, 2319 (1991).
[75] C. Chin, R. Grimm, P. Julienne, and E. Tiesinga, Feshbach resonances in ultracold gases, Rev. Mod. Phys. **82**, 1225 (2010).
[76] V. Efimov, Energy levels arising form the resonant two-body forces in a three-body system, Phys. Lett. B **33**, 563 (1970).
[77] H.-W. Hammer and T. Mehen, A Renormalized equation for the three-body system with short range interactions, Nucl. Phys. A **690**, 535 (2001).
[78] F. Bringas, M. T. Yamashita, and T. Frederico, Triatomic continuum resonances for large negative scattering lengths, Phys. Rev. A **69**, 040702(R) (2004).
[79] A. Deltuva, Energies and widths of Efimov states in the three-boson continuum, Phys. Rev. C **102**, 034003 (2020).
[80] S. Jonsell, Efimov states for systems with negative scattering lengths, Europhys. Lett. **76**, 8 (2006).
[81] T. Hyodo, T. Hatsuda, and Y. Nishida, Universal physics of three bosons with isospin, Phys. Rev. C **89**, 032201(R) (2014).
[82] R. A. Briceno, J. J. Dudek, and R. D. Young, Scattering processes and resonances from lattice QCD, Rev. Mod. Phys. **90**, 025001 (2018).
[83] G. C. Groenenboom, The Discrete Variable Represenation, www.theochem.kun.nl/~gerritg, 2001.
[84] A. Bulgac and M. M. Forbes, Use of the discrete variable representation basis in nuclear physics, Phys. Rev. C **87**, 051301(R) (2013).
[85] S. König, Few-body bound states and resonances in finite volume, Few-Body Syst. **61**, 20 (2020).
[86] S. Elhatisari, E. Epelbaum, H. Krebs, T. A. Lähde, D. Lee, N. Li, B.-N. Lu, Ulf-G. Meißner, and G. Rupak, *Ab initio* Calculations of the Isotopic Dependence of Nuclear Clustering, Phys. Rev. Lett. **119**, 222505 (2017).
[87] M. Yamashita, T. Frederico, and L. Tomio, Three-boson recombination at ultralow temperatures, Phys. Lett. A **363**, 468 (2007).
[88] H.-W. Hammer and D. T. Son, Unnuclear physics, Proc. Natl. Acad. Sci. USA **118**, e2108716118 (2021).